11 August 2000

ELSEVIER

Chemical Physics Letters 326 (2000) 11–21

CHEMICAL PHYSICS LETTERS

www.elsevier.nl/locate/cplett

Survival of HCl($v = 2$) in trapping-desorption from MgO(100)

M. Korolik [1], M.M. Suchan, M.J. Johnson [2], D.W. Arnold [3], H. Reisler *, C. Wittig

Department of Chemistry, University of Southern California, Los Angeles, CA 90089-0482, USA

Received 10 January 2000; in final form 19 May 2000

Abstract

An HCl molecular beam incident on MgO(100) is photoexcited to $v = 2$, $J = 1$ by using a pulsed parametric oscillator. At a translational energy of 0.11 eV, incident HCl is adsorbed. Thermal desorption yields $v = 2$ molecules whose rotational and translational degrees of freedom are equilibrated at the surface temperature. Surface residence times for $v = 2$ might be as long as 1 μs. At 180 K, it is concluded that a large fraction of surface-bound $v = 2$ molecules reenter the gas phase, while at 120 K, deactivation exceeds desorption by an order of magnitude. Deactivation probably takes place at steps.

1. Introduction

Collisions with insulator surfaces, in which the incident molecules contain specific vibrational excitations, have been examined for a number of prototypical systems [1–7]. The majority of this work has been carried out in the direct-inelastic scattering regime, where the incident molecules rebound without sticking. This has led to a good understanding of such processes, at least for small molecules.

When the incident translational energy, E_{inc}, is sufficiently low, the sticking coefficient is near unity. Molecules which stick and subsequently reenter the gas phase are said to be in the trapping-desorption regime. Here, the adsorbed molecules equilibrate with the surface. For smooth metal surfaces, the desorbed molecules can retain some memory of the incident momentum parallel to the surface [8–10]. However, for corrugated surfaces, such as the MgO(100) system under consideration here, this is not the case.

On insulator surfaces, as opposed to metal surfaces [11–13], it is known that adsorbed molecules can retain their vibrational excitation for a long time. This has been studied in detail, most notably by Ewing and co-workers [14]. Thus, it is possible for vibrationally excited incident molecules to be adsorbed on an insulator surface with their vibrational excitation intact. Depending on conditions, they may then be either deactivated or reenter the gas phase by thermal desorption. Deactivation can take place at terrace sites and / or defects, which are mainly steps in the case of MgO(100), but little is known about the deactivation sites and mechanisms.

In this Letter, experimental results are presented which demonstrate that surface-bound HCl molecules

* Corresponding author. Fax: +1-213-746-4945; e-mail reisler@chem1.usc.edu

[1] Present address: Silicon Genesis Corporation, 590 Division St., Campbell, CA 95008.

[2] Present address: Continuum, Inc., Unit 32, #1 Beach Road, Bondi Beach, Sydney, Australia 2026.

[3] Present address: Sandia National Laboratory, Mail Stop 9671, Livermore, CA 94551-0969.

0009-2614/00/$ - see front matter
PII: S0009-2614(00)00690-4

in $v = 2$ retain their vibrational excitation for a long time. Namely, they can be thermally desorbed with their $v = 2$ excitation intact. Above ~ 160 K, our tentative conclusion is that the majority of the $v = 2$ molecules reenter the gas phase, while at 120 K, the deactivation rate is an order of magnitude larger than the desorption rate. It will be argued that the most likely deactivation mechanism is diffusion to defects, where $v = 2$ deactivation occurs without producing a significant number of gas phase $v = 1$ molecules.

2. Experimental

The experimental arrangement is shown in Fig. 1. Pulsed molecular beams containing HCl were prepared by using supersonic expansions of HCl dilute in suitable carriers [15]. The expansion-cooled HCl was promoted to the $v = 2$, $J = 1$ state by using a pulsed infrared optical parametric oscillator (OPO). These excited molecules impinged on a MgO(100) surface, and the resulting state and time-of-flight (TOF) distributions of the scattered $v = 1$ and 2 molecules were obtained by using quantum-state-selective laser detection, as described below. The experiments were performed at different values of E_{inc} and surface temperatures, T_s. The former was adjusted via the gas mixtures, e.g., 1–2% HCl in 2 atm. of H_2 or Ne at 300 K yields E_{inc} values of 0.90 or 0.11 eV, respectively.

A piezoelectric nozzle (20 Hz, ~ 200 μs pulse duration) was used to create the pulsed expansion. After traversing a differentially pumped region, the molecular beam entered the UHV chamber (base pressure 3×10^{-10} Torr) which housed the MgO crystal. The surface was prepared by cleaving MgO along the (100) plane prior to mounting it on an XYZ manipulator and placing it in the UHV chamber. In order to minimize contaminants and oxygen deficiencies, the crystal was heated to 500°C for several hours in 10^{-5} Torr of O_2. Auger spectroscopy was used to check surface cleanliness on a daily basis and surface order was verified by using He diffraction.

The expansion-cooled $H^{35}Cl$ was photoexcited from the $v = 0$, $J = 0$ ground state to $v = 2$, $J = 1$. The source of the radiation used in this step was a KTP OPO whose output was amplified in two KTP crystals. The oscillator and amplifiers were pumped with the second harmonic of an injection-seeded Nd:YAG laser, yielding 5 ns pulses near 1.73 μm (linewidth ~ 0.01 cm^{-1}, energies ~ 4 mJ). A

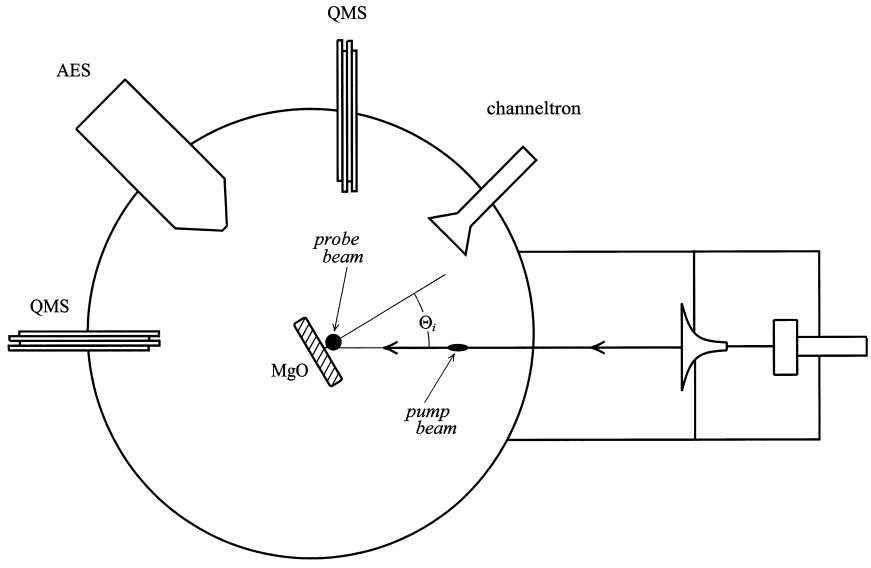

Fig. 1. Schematic of the experimental arrangement. AES and QMS refer to Auger electron spectrometer and quadrupole mass spectrometer, respectively. Θ_i is the angle of incidence.

photoacoustic signal was used to match the OPO frequency to the desired HCl overtone transition; the frequency was maintained at line center by using a custom-built frequency stabilization system [16].

HCl molecules were detected state-selectively by using (2 + 1) resonance-enhanced multiphoton ionization (REMPI). To obtain the required radiation, the output of a dye laser was frequency doubled in BBO to generate tunable radiation in the range 250–254 nm having a linewidth of approximately 0.12 cm^{-1} and an energy of 3–4 mJ. HCl($v = 2$) was detected by using Q branch transitions of the $V^1\Sigma^+(v = 12) \leftarrow X^1\Sigma^+(v = 2)$ band ($\sim$ 253 nm) as the two photon step. These transitions have been shown to yield signals which are larger than those which derive from transitions whose upper states are $V^1\Sigma^+(v = 11)$, $E^1\Sigma^+(v = 0)$ [17] and $F^1\Delta(v = 1)$ [18] by factors of roughly 2, 4, and 10, respectively. The signals were normalized to the square of the laser energy, because the ionization step is saturated, while the two-photon step is not. Rotational line strengths for Q branch transitions of the $V^1\Sigma^+(v = 12) \leftarrow X^1\Sigma^+(v = 2)$ band were assumed to be unity. HCl($v = 1$) was detected with $\sim$ 250 nm radiation by using Q branch transitions of the $V^1\Sigma^+(v = 9) \leftarrow X^1\Sigma^+(v = 1)$ system. To calibrate the probe laser frequency, rotational levels within $v = 2$ and 1 were detected following $v = 2$, $J = 1$ photoexcitation in an ion cell filled with HCl. Rotational energy transfer within $v = 2$ was observed at a pump-probe delay of 100 ns (at pressures $\sim$ 0.2 Torr), while the $v = 1$ concentration increased for delays longer than 1 μs (at pressures $\sim$ 20 Torr).

Referring to Fig. 1, the OPO beam crossed the molecular beam at a right angle 2–6 mm from the surface, while the probe laser beam crossed the plane of incidence at a right angle 0.5–5 mm from the surface. By scanning the delay between the OPO and the probe laser, temporal profiles of the incident molecules and time-of-flight (TOF) distributions of the scattered molecules were recorded. The temporal width of the packet of vibrationally excited HCl molecules in the incident beam depended on the OPO focusing conditions and the velocity characteristics (i.e., average value and spread) of the HCl in the molecular beam. Temporal profiles of incident $v = 2$, $J = 1$ as short as 200 ns FWHM were obtained for HCl having $E_{inc} = 0.90$ eV. For $E_{inc} = 0.11$ eV, the temporal profile of incident $v = 2$, $J = 1$ was 1.5 μs FWHM. These narrow temporal profiles of the incident molecules allowed the TOF technique to be used to determine translational energy distributions of scattered molecules. Flux to density transformation and convolution over incident temporal profiles were used in the analysis of the TOF spectra. It was also possible to obtain incident pulses with durations of approximately 15 μs ($E_{inc} = 0.11$ eV) by focusing the OPO along the molecular beam axis with a cylindrical lens.

3. Results

The spatially and temporally resolved preparation of incident HCl($v = 2$, $J = 1$) molecules provides an excellent starting point for the state-resolved examination of a number of inelastic scattering processes. For example, because of the background-free nature of the measurements, it is possible to probe the vibrationally elastic (but rotationally inelastic) $v = 2 \rightarrow v = 2$ channel, as well as the vibrationally inelastic $v = 2 \rightarrow v = 1$ channel. In addition, it is possible to verify and examine rather long $v = 2$ surface residence times, i.e., very much longer than an HCl vibrational period. These long residence times are the main focus of the present paper.

Following collisions of the incident $v = 2$, $J = 1$ molecules with the surface, rotational state distributions of the scattered $v = 2$ molecules were obtained for different values of experimental parameters such as E_{inc} and T_s. Referring to Fig. 1, the angle of incidence, Θ_i, was maintained at approximately 15° in all of the experiments.

3.1. High energy collisions: $E_{inc} = 0.90$ eV

Fig. 2a shows a REMPI spectrum which is typical of those used to monitor $v = 2$; T_s is 300 K and the surface–probe distance is 2–3 mm. $E_{inc} = 0.90$ eV is large relative to the binding energy for HCl on MgO(100), as discussed below. Such spectra provide distributions of the HCl rotational states within $v = 2$. For the data shown in Fig. 2a, the rotational state distribution obtained from the Q branch line intensities compares favorably to a 400 K Boltzmann distribution, as shown in the inset.

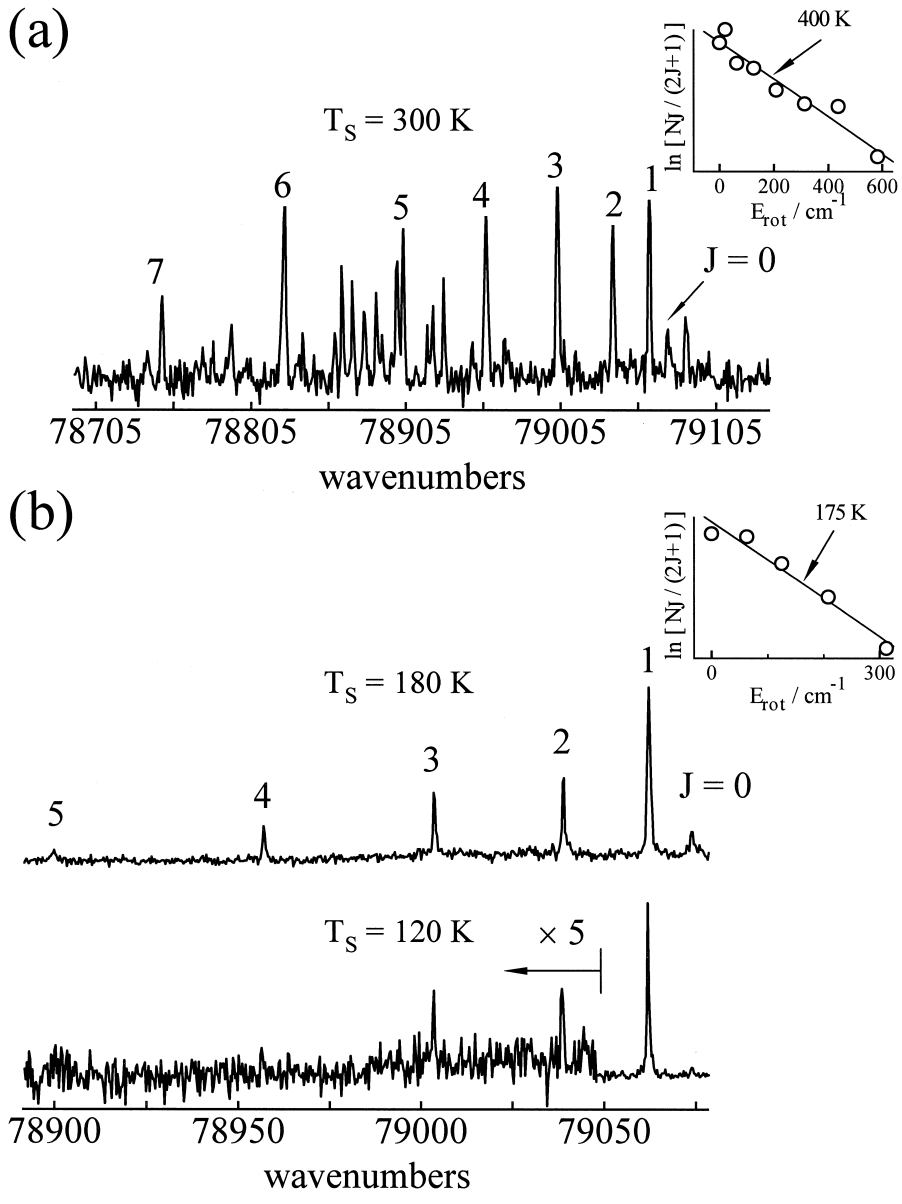

Fig. 2. REMPI spectra of HCl($v = 2$) scattered from MgO(100): (a) $E_{inc} = 0.90$ eV; $T_s = 300$ K. (b) $E_{inc} = 0.11$ eV; $T_s = 180$ K (upper) and 120 K (lower). Boltzmann plots are upper right inserts.

TOF distributions for $v = 2$, $J = 4$ molecules which derive from the molecule-surface collision were recorded at $T_s = 300$ K and surface–probe distances of 1.0 and 1.5 mm, as shown in Fig. 3a. The temporal profile of the incident $v = 2$, $J = 1$ molecules is shown in the upper left. The $v = 2$, $J = 4$ widths are considerably larger than that of the incident molecules, reflecting the velocity distribution which results from the molecule-surface interaction.

The tails of the TOF distributions are due, at least in part, to the angular distribution of the scattered molecules. Namely, molecules which are scattered out of the plane of incidence travel a larger distance

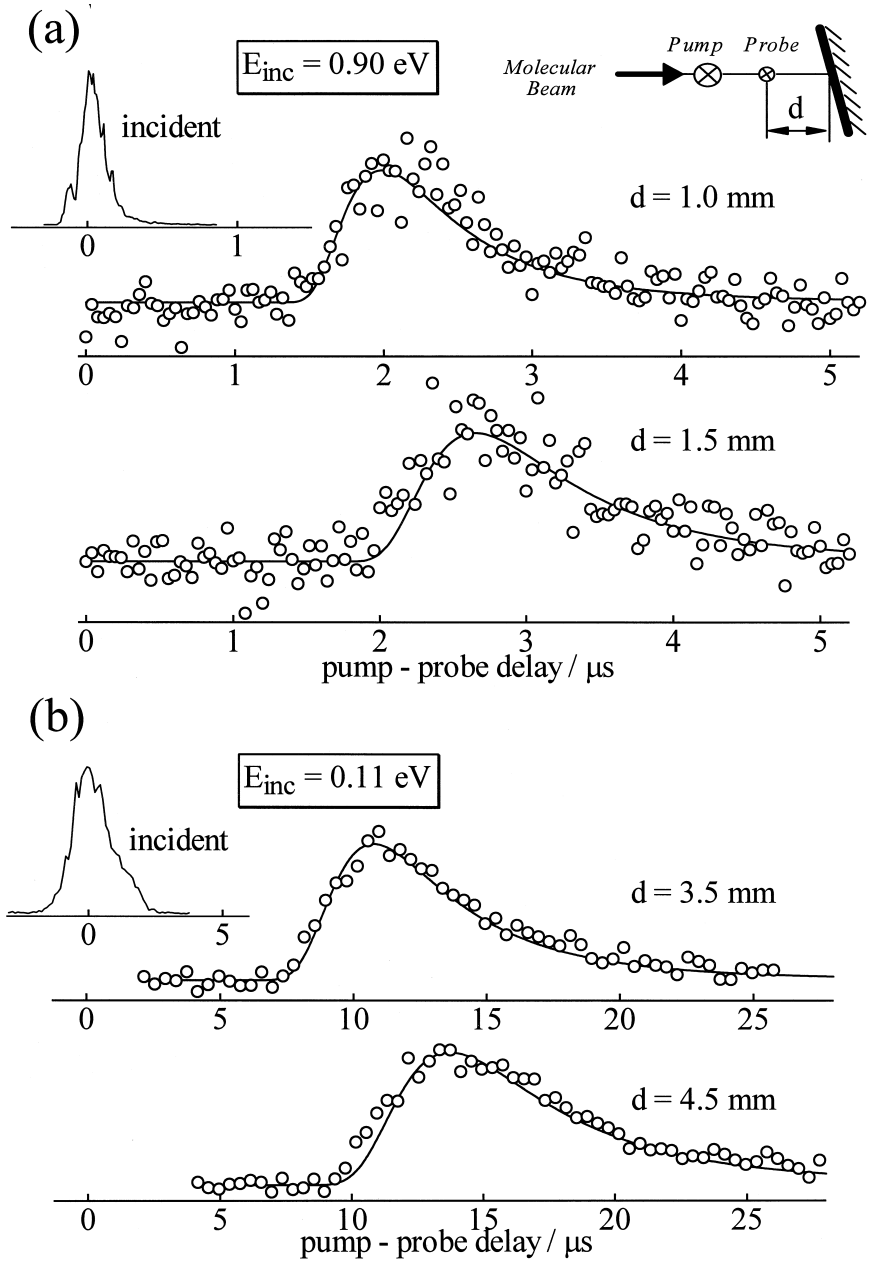

Fig. 3. Temporal profiles of HCl ($v = 2,\ J = 4$): (a) $E_{inc} = 0.90$ eV and $T_s = 300$ K. Incident, HCl($v = 2,\ J = 1$) is shown in the upper left. Probe-surface distances are 1 and 1.5 mm, as indicated in the upper right. (b) $E_{inc} = 0.11$ eV, $T_s = 390$ K. The TOF distributions are recorded at probe-surface distances of 3.5 and 4.5 mm. The solid curves correspond to model distributions.

before encountering the probe radiation than those which remain in the plane of incidence. Analysis of the TOF spectra indicates that the $v = 2,\ J = 4$ molecules which leave the surface have a broad translational energy distribution with a mean value of ~ 0.4 eV, which is far in excess of $2kT_s$. This confirms the dominance of a direct-inelastic scattering mechanism at $E_{inc} = 0.90$ eV.

3.2. Low energy collisions: $E_{inc} = 0.11$ eV

Fig. 2b shows REMPI spectra for $E_{inc} = 0.11$ eV and T_s values of 180 K (upper entry) and 120 K (lower entry). This E_{inc} value is less than the binding energy for HCl on MgO(100), as discussed below. The surface–probe distance was approximately 1 mm. Some $v = 2$, $J = 1$ incident molecules were in the detection region at the time when the scattered molecules were probed, giving rise to a relatively large REMPI signal at $J = 1$. The experiments carried out at $T_s = 120$ and 180 K were performed under otherwise identical conditions, including the probe position and the pump-probe delay. Consequently, the signal intensities which are due to incident $v = 2$, $J = 1$ were equal under the same expansion conditions, thereby providing a convenient means of normalization.

The rotational state distribution for $T_s = 180$ K compares favorably to a 175 K Boltzmann distribution (excluding $J = 1$), as shown in the inset. The data at $T_s = 120$ K could not be fit because of the low signal level. The different signal levels for 180 and 120 K is striking. The scattered $v = 2$ signal decreases by an order of magnitude as T_s decreases from 180 to 120 K.

TOF distributions for $v = 2$, $J = 4$ were recorded for $T_s = 390$ K and surface–probe distances of 3.5 and 4.5 mm, as shown in Fig. 3b. The temporal profile of the incident $v = 2$, $J = 1$ molecules is shown in the upper left. When the probe laser was positioned further from the surface, the scattered molecules arrived later at the detection region and the TOF distribution was broader. These TOF data can be fit by using a Maxwell–Boltzmann velocity distribution at T_s.

To examine the effect of the surface residence time on the TOF distributions, the temporal profile of $v = 2$, $J = 2$ was recorded for $T_s = 160$ K and a surface–probe distance of 1 mm, as shown in Fig. 4a. The profile follows that of the incident pulse. There is no tail extending to long times, in contrast to the scattered $v = 0$ profiles reported earlier and shown in Fig. 5 [15]. Note that the time scale of the $v = 0$ profiles is two orders of magnitude longer than that of the $v = 2$ experiments reported here. At 120 K, the temporal shape (Fig. 4b) is about the same as at 160 K. However, the signal level is down by an order of magnitude.

The $v = 1$ deactivation product was detected for $1 \leq J \leq 4$. However, the signal level was lower than that of $v = 2$ by an order of magnitude. By focusing the OPO radiation to a line with a cylindrical lens, the largest possible number of $v = 2$ molecules was generated, and this enabled TOF distributions to be obtained (Fig. 4c). As with the $v = 2$ data shown in

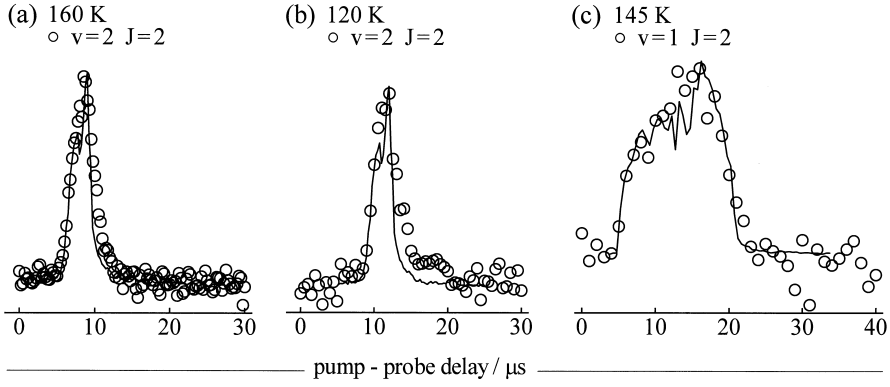

Fig. 4. At $E_{inc} = 0.11$ eV, the temporal profiles of desorbed molecules recorded near the MgO(100) surface have essentially the same shape as the incident pulses. The solid lines are temporal profiles of incident HCl($v = 2$, $J = 1$) molecules recorded without a surface present and shifted to longer times to account for the flight time. The probe-surface distance is approximately 1 mm. (a) At $T_s = 160$ K most surface-bound $v = 2$ molecules enter the gas phase. (b) At $T_s = 120$ K most of the $v = 2$ molecules are deactivated on the surface. (c) For monitoring $v = 1$, the incident pulse was lengthened.

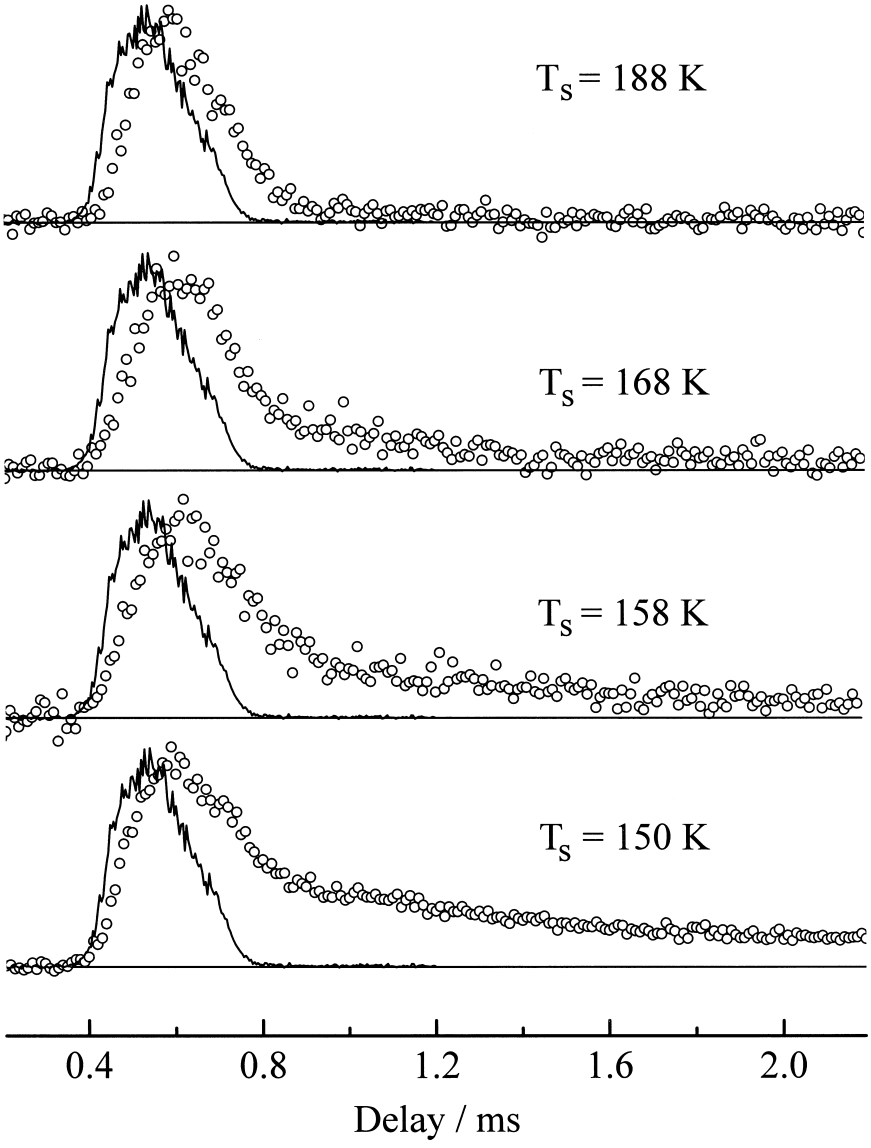

Fig. 5. Temporal profiles: incident HCl ($v = 0$, $J = 0$) (solid line) and scattered HCl ($v = 0$, $J = 2$) (open circles) at $E_{inc} = 0.11$ eV and $\Theta_i = 15°$ for different values of T_s. Taken from Ref. [15].

Figs. 4a and 4b, the $v = 1$ temporal profile followed that of the incident pulse.

4. Discussion

The main results of this paper are the observation of long survival times of HCl($v = 2$) on MgO(100) and the changes of the scattered signal intensity and the TOF spectra with T_s. Specifically, $v = 2$ molecules can reside on the surface for times which may be as long as 1 μs (our TOF resolution), equilibrating their rotational and translational degrees of freedom with the surface, and the scattered HCl($v = 2$) signal intensity decreases by an order of magnitude when T_s decreases from 180 to 120 K.

These results can be compared to the behavior of scattered HCl in $v = 0$ at similar E_{inc} and T_s, but with a molecular beam pulse duration of ~ 300 μs.

In the previous results (Fig. 5), the TOF spectra obtained at low T_s showed two components: an early one that followed the molecular beam pulse, and a long tail, which extended to > 1 ms. It is reasonable that the long tails are for molecules adsorbed at defects, whereas the early components are due to terrace sites. An activation energy for desorption from defects, E_{def}, of approximately 0.3 eV was obtained from the long tail by using the usual expression for the desorption rate,

$$k_{desorb} = \nu_0 e^{-E_{def}/kT_s} \quad (1)$$

with $\nu_0 = 10^{13}$ s^{-1}, which is typical for atomic adsorbates [19]. ν_0 will be slightly higher for the physisorbed HCl due to the entropy increase experienced by HCl upon going from the geometrically constrained desorbed state to the gas phase [20]. [Note that for a ν_0 value of 10^{14} s^{-1}, the E_{def} value is only slightly larger, i.e., 0.33 eV.] As stated above, the defects are mainly step edges, which are common for cleaved MgO(100) crystals, and are typically separated by several hundred Angstroms [21,22]. They constitute regions of enhanced reactivity, and the adsorbed HCl molecules, which initially land mostly on terrace sites, will migrate towards the steps, where their residence time is longer [23,24].

Surface-bound HCl($v = 2$) molecules can be deactivated with a rate coefficient, k_{deact}, which represents deactivation at terrace and / or defect sites. On terraces, the temperature dependence of k_{deact} is expected to be modest relative to that of k_{desorb}. Thus, k_{deact} is assumed to be nearly constant over the 120–180 K temperature range which has been used to vary k_{desorb} in the present work.

Our observations are consistent with a model that assumes that HCl($v = 2$) is deactivated predominantly at defect sites, rather than on terraces. Below we describe the model and compare it briefly to a scenario that involves deactivation only at terrace sites.

The rate equation for surface-bound $v = 2$ molecules is:

$$\frac{dN}{dt} + kN = \Phi(t), \quad (2)$$

where N is the concentration of surface-bound $v = 2$ molecules, $\Phi(t)$ is the incident $v = 2$ flux, and $k = k_{deact} + k_{desorb}$. The solution to Eq. (2) is:

$$N(t) = \int_{-\infty}^{t} dt' e^{-k(t-t')}\Phi(t'). \quad (3)$$

Once $N(t)$ is known, the flux of $v = 2$ molecules into the gas phase is readily obtained by multiplying $N(t)$ by k_{desorb}.

An important consideration is how the excited HCl molecules, which land predominantly on terrace sites, find their way to the defects. It is thought that for low defect densities, the defects are reached by random walk, a process that has a marked temperature dependence because it is controlled by the hopping rate between terrace sites [20,24,25]. This hopping rate can be expressed as $\nu_{hop}\exp\{-E_{hop}/kT_s\}$, where ν_{hop} is expected to be comparable to ν_0, and E_{hop} is the energy of the barrier to hopping between terrace sites. Thus, as T_s is lowered, the hopping rate (and consequently the diffusion rate) decreases.

It is possible to get a rough estimate of the average distance the molecules diffuse away from their landing site, $\langle l \rangle$, by using a random walk model that gives

$$\langle l \rangle \propto (Dt)^{1/2}, \quad (4)$$

where D is the diffusion coefficient, which is related to the hopping rate, and t is the elapsed time. Eq. (4) gives an average diffusion length which is proportional to $\exp\{(E_{ter} - E_{hop})/2kT_s\}$. E_{ter} is the barrier to desorption from *terrace* sites, which determines the rate of reentry to the gas phase of those HCl($v = 2$) molecules that did not reach a defect site. Since E_{hop} is smaller than E_{ter}, the average diffusion length on the terraces increases as T_s decreases. Put differently, the probability of reaching a defect site increases with decreasing T_s, and thus the effective deactivation rate coefficient will be temperature dependent (assuming that every molecule that reaches a defect site is deactivated). A detailed analysis will be published in a full account of our results, but we note here that our model is similar to the one invoked to describe the behavior of adsorbed NO_2 on GaAs surfaces, where defects serve as dissociation sites [24].

The main obstacle to a quantitative implementation of this model is our ignorance of the parameters

E_{ter} and E_{hop}. As discussed below, E_{ter} is ~ 0.2 eV. For metal surfaces, it is known that E_{hop} is usually between 0.1 and 0.25 of E_{ter}, while for insulator surfaces, E_{hop} will be a larger fraction of E_{ter}. However, we are not able to estimate E_{hop} for the present system, though similar systems provide some qualitative guidance [21]. By making the assumption that the value of E_{hop} ranges between 0.2 and 0.4 of E_{ter}, the dependence of $\langle l \rangle$ on T_s can be estimated. Assuming that the average distance between steps is $\sim 5 \times 10^2$ Å [22], we obtain a dependence of the scattered HCl($v = 2$) signal intensity and residence time on T_s that is consistent with our observations. For example, we find that at $T_s = \sim 150$ K, the diffusion length exceeds the distance between steps, and that the increase in the fraction of molecules that reach the defects sites with decreasing temperature can explain the observed signal intensity dependence.

There have been no direct experimental measurements of the binding energy for HCl on MgO. Chacon-Taylor and McCarthy [26] have used ab initio methods and obtained a value of 0.48 eV, while the value obtained by electrostatics is ~ 0.25 eV. The binding energy for terrace sites will be lower than 0.3 eV, though it has not been possible to obtain an estimate of its value in our earlier work [15]. We believe that it should not be too much lower than the value estimated by using electrostatics, which appears to account for most of the binding energy in of adsorbantes on MgO(100) [21]. The value of E_{ter} that we use, ~ 0.2 eV, is close to that obtained for HCl and other small molecules by electrostatics [21,26,27]. It is compatible with deactivation occurring mostly at defects and with a residence time of ~ 1 μs.

The finding that for desorbed molecules the $v = 1$ population is small relative to the $v = 2$ population is consistent with deactivation taking place at defects, where the binding energy and chemical forces are larger than at terrace sites. For example, deactivation of $v = 2$, yielding $v = 1$, liberates approximately 0.35 eV, which is close to $E_{def} = 0.3$ eV. Thus, it is anticipated that it will be difficult for $v = 1$ to enter the gas phase. On the other hand, it is easier for the $v = 1$ deactivation product to enter the gas phase when deactivation takes place on the terrace, because E_{ter} is ~ 0.2 eV.

We now compare our results to a model in which vibrational deactivation takes place predominantly at terrace sites. If defects played no significant role in the system under consideration, the surface bound $v = 2$ molecules would experience only two fates: desorption from the terrace, characterized by k_{desorb}, and deactivation at the terrace, characterized by a rate coefficient k_{deact}, which is taken to be constant over the 120–180 K temperature range.

We first note that it is not possible to reconcile the present results with an E_{ter} value of 0.3 eV. Specifically, at $T_s = 120$ K, Eq. (3) gives a surface residence time of 0.4 s, which is incompatible, by 4 orders of magnitude, with the data.

For $E_{ter} \sim 0.2$ eV, k_{desorb} decreases by three orders of magnitude as T_s goes from 180 to 120 K. However, the measured intensity of $v = 2$ that leaves the surface decreases by only one order of magnitude in this T_s range. In addition, k must be $\geq 10^6$ s^{-1} throughout this T_s range, because there is no significant spreading of the TOF spectra relative to the incident beam pulse (Fig. 4).

Although the above requirements can be met by using numerous combinations of k_{desorb} and k_{deact}, it is not possible to have $k_{deact} \geq k_{desorb}$ at $T_s = 180$ K. If it were, the loss of signal as T_s decreases from 180 to 120 K would far exceed what has been observed experimentally. For $k_{deact} \leq k_{desorb}$ at 180 K, it is possible to choose values such that the signal decreases by only one order of magnitude. However, it will do so over a much smaller T_s interval, e.g., between 120 and 135 K. The data show a less pronounced variation of signal versus T_s. However, given the rough estimates enlisted here as well as the imprecision of the data, we are remiss to rule out this possibility, though we deem it less probable than the mechanism involving defects as the major deactivation sites.

5. Conclusions

At $E_{inc} = 0.90$ eV, incident HCl($v = 2$) molecules mainly undergo inelastic scattering. In light of previous research on such processes, the results are not surprising.

At $E_{inc} = 0.11$ eV, incident HCl($v = 2$) molecules: (i) are adsorbed onto a MgO(100) surface; (ii) are

thermalized in every respect except one, i.e., retention of their $v = 2$ excitation; and (iii) reenter the gas phase by thermal desorption with their $v = 2$ excitation intact. The residence times of the surface-bound $v = 2$ molecules can be long. At the higher T_s values, $v = 2$ residence times are dictated by desorption from terrace sites. At the lower T_s values, we propose that diffusion to defects facilitates deactivation.

It has not been possible to establish the mechanism unambiguously. Our tentative conclusion is that at $T_s = 180$ K there is little deactivation of surface bound $v = 2$. Most of these species enter the gas phase. At $T_s = 120$ K, the deactivation rate is an order of magnitude larger than the desorption rate. Deactivation probably occurs mainly at defects.

The conclusion that for $T_s \geq 180$ K the majority of the incident $v = 2$ molecules reenter the gas phase with their vibrational excitation intact has been inferred as follows. First, the amount of $v = 2$ emerging from the surface at $E_{inc} = 0.11$ eV is approximately constant from $T_s = 180$ to 300 K (the highest temperature examined). Were surface-bound $v = 2$ deactivated to a significant extent, increasing T_s over this range would increase the signal due to the shortening of the residence time. If, at 180 K, the deactivation of $v = 2$ is more efficient than desorption, the loss of signal in going to 120 K would be *several* orders of magnitude.

Second, though it is not possible with our current configuration to determine quantitatively the respective amounts of incident and scattered $v = 2$, an order of magnitude estimate can be made. In monitoring $v = 2$, $J = 2$, only 20–25% of the scattered $v = 2$ molecules are probed, whereas 100% of the incident $v = 2$, $J = 1$ molecules are probed. In addition, the angular distribution of scattered $v = 2$ is such that only about 15% of the flight paths of the scattered molecules are intercepted by the probe. Also, in some cases the $v = 2$ temporal profile has spread relative to that of $v = 2$ in the incident beam. The large differences in S/N between incident and scattered molecules can be rationalized by taking the above factors into account, leading to the conclusion that the amount of scattered $v = 2$ is of the same order of magnitude as the amount of incident $v = 2$.

The tentative conclusions presented in this paper will be tested in future experiments. For example, molecules such as CO_2 can be used to decorate the defects, perhaps lengthening $v = 2$ residence times, and facilitating studies of state-selective reactive and inelastic scattering on the terrace. In addition, the molecules which decorate the defects may themselves be attractive targets for studies of site-specific chemistry, for example photoinitiated reactions.

Acknowledgements

The authors benefited from discussions with J. Tully, W. Kim, S. Hawkins, and B.E. Koel. This research was supported by the Air Force Office of Scientific Research.

References

[1] J. Misewich, H. Zacharias, M.M.T. Loy, Phys. Rev. Lett. 55 (1985) 1919.
[2] H. Zacharias, M.M.T. Loy, P.A. Roland, Phys. Rev. Lett. 52 (1982) 1790.
[3] J.S. Hamers, P.L. Houston, R.P. Merrill, J. Chem. Phys. 92 (1990) 5661.
[4] H. Vach, J. Hager, H. Walther, J. Chem. Phys. 90 (1989) 6701.
[5] R.T. Jongma, G. Berden, T. Rasing, H. Zacharias, G. Meijer, Chem. Phys. Lett. 273 (1997) 147.
[6] J. Arnold, T. Bouche, T. Dreier, J. Wichmann, J. Wolfrum, Chem. Phys. Lett. 203 (1993) 283.
[7] A.C. Wight, M. Penno, R.E. Miller, J. Chem. Phys. 111 (1999) 8622.
[8] C.T. Rettner, Surf. Sci. 204 (1988) L677.
[9] M.E.M. Spuit, P.J. v.d. Hoek, E.W. Kuipers, F.H. Geuzebroek, A.W. Kleyn, Phys. Rev. B 39 (1989) 3915.
[10] C.T. Rettner, J.A. Barker, D.S. Bethune, Phys. Rev. Lett. 67 (1991) 2183.
[11] J. Misewich, P.L. Houston, R.P. Merrill, J. Chem. Phys. 82 (1985) 1577.
[12] M. Gostein, E. Watts, G.O. Sitz, Phys. Rev. Lett. 79 (1997) 2891.
[13] A. Hodgson, P. Samson, A. Wight, C. Cottrell, Phys. Rev. Lett. 78 (1997) 963.
[14] G.E. Ewing, Acc. Chem. Res. 25 (1992) 292.
[15] M. Korolik, D.W. Arnold, M.J. Johnson, M.M. Suchan, H. Reisler, C. Wittig, Chem. Phys. Lett. 284 (1998) 164.
[16] W.R. Bosenburg, D.R. Guyer, J. Opt. Soc. Am. B 101 (1993) 1716.
[17] P.T.A. Reilly, Y. Xie, R.J. Gordon, Chem. Phys. Lett. 178 (1991) 511.
[18] C.T. Rettner, J. Chem. Phys. 101 (1994) 1529.
[19] A. Zangwill, Physics at Surfaces, Cambridge University Press, 1988.

[20] J.C. Tully, Surf. Sci. 299/300 (1994) 667.
[21] S. Briquez, A. Lakhlifi, S. Picaud, C. Girardet, Chem. Phys. 194 (1995) 65.
[22] C. Duriez, C. Chapon, C.R. Henry, J.N. Rickard, Surf. Sci. 230 (1990) 123.
[23] J.A. Serri, J.C. Tully, M.J. Cardillo, J. Chem. Phys. 79 (1983) 1530.
[24] C.C. Bahr, A. vom Felde, S.K. Buratto, M.J. Cardillo, J. Chem. Phys. 102 (1995) 4452.
[25] R. Gomer, Rep. Prog. Phys. 53 (1990) 917.
[26] M.R. Chacon-Taylor, M.I. McCarthy, J. Phys. Chem. 100 (1996) 7610.
[27] S. Briquez, C. Girardet, J. Goniakowski, C. Noguera, J. Chem. Phys. 105 (1996) 678.